Chapter 5

Neuroimaging, Biochemical investigation with causal analysis of hepatometabolic agents for Alzheimer's disease

Chapter 5

5. Neuroimaging, Biochemical investigation with causal analysis of hepatometabolic agents for Alzheimer's disease

5.1 Introduction

Liver and its lipid homeostasis play vital role in Alzheimer's disease. Cholesterol metabolism in liver has crucial effect on amyloid-beta clearance through cerebral vasculature. Ageing-induced hepatic dysfunction can impair cholesterol metabolism, reducing the availability of cholic-acid (CA, primary bile acid) in brain. CA is reported to have neuroprotective characteristics in preclinical investigations of Alzheimer's disease. Our aim is to probe the interaction and causational relationship between the players: amyloid, cholic acid and cerebral blood flow in the human context.

We analysed serum cholic-acid concentrations for 182 healthy and 136 Alzheimer's disease subjects from the biospecimen platform of Alzheimer's disease neuroimaging initiative to examine link between alteration of bile acid profile and cognitive impairment. We selected (i) 50 healthy and 50 Alzheimer's subjects containing both MRI-ASL scanning (quantifies cerebral blood flow, CBF) and PET-AV45 scanning (quantifies amyloid-beta load) from the aforesaid platform, (ii) 50 healthy subjects from the OASIS-3 platform. We evaluated the interactions of cholic acid levels with CBF and amyloid load (SUVR), and also performed Granger causality (GC) analysis to determine the cause-effect relationship among the parameters.

Statistical analysis revealed the serum cholic acid in Alzheimer's subjects especially significantly decreases to half of the value in normal subjects ($p = 0.0053$). Moreover, brain amyloid load in Alzheimer's subject is significantly higher than normal subjects ($p < 0.0001$). Further, total and regional cerebral blood flow (precuneus, hippocampus, and cingulate cortex) in Alzheimer subjects diminishes substantially by 45-

50% of normal values ($p < 0.0001$). However, within healthy subjects, the alteration of amyloid-beta load did not correlate with cerebral blood flow ($p=0.1265$), which may be due to subthreshold variation. Regression analysis revealed there was significant interaction of cholic-acid level with amyloid load ($p = 0.0496$) and CBF ($p < 0.0001$). The Cohen's effect size index ($f^2 \geq 0.42$) indicates the manifestation of large effect size in both amyloid load and CBF. Our Causation Analysis revealed that (i) decrease of serum cholic acid markedly increases amyloid-beta load ($p = 0.01$), and (ii) the increase in amyloid-load markedly decreases cerebral blood flow ($p = 0.02$).

We investigated Alzheimer's disease from a metabolic perspective, showing the significance of the body's basic metabolic system, the hepatobiliary framework and its metabolites. Thus, repositioned pharmacological modulation by cholate derivatives or cholic acid may have appreciable potentiality as a novel window for therapeutic approach to Alzheimer's disease, and already available indicative clinical trial leads are delineated.

5.2 Materials and methods

5.2.1 Scanning of Alzheimer's Disease patients

In the present study, we have utilized scanning images from the Alzheimer's Disease Neuroimaging Initiative program (ADNI). The ADNI program was launched in 2004 as an multicentric clinical cooperation as a private-public partnership. The principal objective of this initiative was to develop clinical, imaging, genetic, and biochemical biomarkers for the early detection and monitoring of Alzheimer's disease (AD).

5.2.2 Serum Cholic Acid Concentration Analysis

We have collected serum cholic acid concentrations for 182 cognitively normal and 136 Alzheimer's disease subjects from the ADNI Biospecimen undertaking. Detailed information regarding standard operating procedure is available in www.adni-info.org. Cholic acid concentration measurement was performed by a UPLC (ultra-high pressure

liquid chromatography) tandem mass spectrometry (MS) method using a reversed phase analytical column for analyte separation using the Biocrates Life Sciences Bile Acids Kit (Biocrates Life Science AG, Innsbruck, Austria) [99].

5.2.3 Scanning of healthy normal subjects

Scanning images has been obtained from Open Access series of Imaging Studies program (OASIS-3) [100] at the Alzheimer's Disease Research Centre. Participants include 605 cognitively normal adults and 493 individuals at various stages of cognitive decline ranging in age from 42 to 95 years. We have, using random sampling, selected 50 cognitively normal subjects containing both ASL and PET AV45 images for this study.

5.2.4 Imaging investigations

Participants chosen for our study were cognitively normal from the OASIS-3 program, and both healthy and Alzheimer diseased older adults from the ADNI-ASL program. All participants included were between 55 and 90 years old, had completed at least six years of education, were fluent in the local language (English or Spanish), and were free of any significant neurological disease other than AD. ADNI control participants (healthy subjects) had Mini-Mental Status Examination (MMSE) scores of 24-30 and a Clinical Dementia Rating (CDR) score of 0. Similarly, for Alzheimer's subjects, MMSE score was between 20-26 and CDR of 0.5-1.0. The Institutional Review Board approved this study of all of the participants. Informed written consent was obtained from all subjects. A total of 100 subjects was included: 50 healthy controls and 50 Alzheimer subjects who were assessed by both the MRI-ASL and PET imaging examination.

5.2.5 Amyloid Load: Florbetapir PET Data Acquisition and Processing

A detailed description of ADNI florbetapir PET imaging data acquisition and processing can be found online (https://adni.loni.usc.edu/methods/pet-acquisition/). Structural T1 images were skull-stripped, segmented, and parcellated using FreeSurfer, and

subsequently co-registered to each participant's PET image. Masks were created for the regions of interest, and then those masks were transformed into the subject space.

For intersubject comparison, we performed intensity normalization of PET images by using the average of pons and cerebellum activity (these regions are conventionally taken as standard baseline, as they have minimal amyloid deposition). Henceforth, we have transformed the normalized image to MNI space, and apply partial volume correction (PVC). This PVC is executed to restrict the activity within the cortex; indeed, the cortical region has definitive amyloid load and is our region of interest. The iterative Yang algorithm [101] implemented in PETPVC [102] was chosen for computational efficiency. Then we used partial volume corrected PET images to obtain amyloid load (SUVR) for the different ROIs (Figure 24). The script containing all the steps discussed above to calculate regional values of the Standard Uptake Value Ratio (SUVR) from the Positron Emission Tomography (PET) scans was made available in the GitHub repository (https://github.com/pratik-purohit/PET_SUVR).

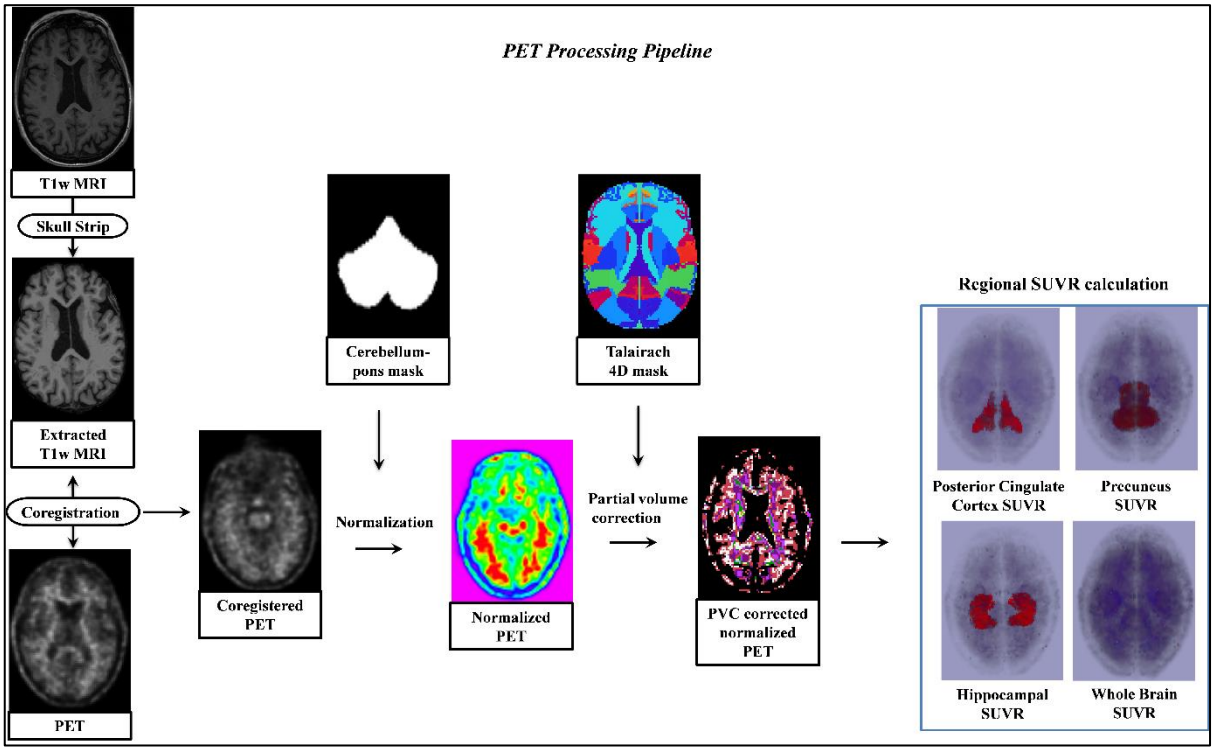

Figure 24: *Image analysis methodology (amyloid PET scanning evaluation).*

5.2.6 Cerebral Blood Flow - MRI Arterial Spin Tagging analysis

The MRI scans were taken with magnetic field strength of 3 Tesla. Quantitative imaging of perfusion using single subtraction second version protocol (QUIPSS II) was utilized to acquire a resting-state pulsed ASL scan [103]. The sequence included the following parameters: Inversion time of arterial spins (TI1): 700 ms, Total transit time of the spins (TI2): 1900 ms, Tag thickness: 100 mm, Tag to proximal slice gap: 25.4 mm, Repetition time: 3400 ms, Echo time: 12 ms, Field of view: 256 mm, 64×64 matrix, 244 mm thick axial slices [52 tag + control image pairs], Time lag between slices: 22.5 ms.

ASL image processing was done utilizing the ExploreASL pipeline (http://www.exploreasl.org). Briefly, the pipeline involves four modules. First was the Import Module, which creates Brain Imaging Data Structure (BIDS) for NIfTI and DICOM formats. It automatically detects the order of control and label images from the image intensities and checks the DICOM tags of repetition, echo time and scale factors/slopes across individuals. The second is the Structural Module, which included correcting white matter hyperintensities, segmentation, and spatial normalization. The third module, the ASL Module, incorporated motion correction, outlier removal, registration with structural data, and M0 image processing. Then the cerebral blood flow (ml/100g brain tissue/minute) is quantified with correction for hematocrit and vascular artifacts, after which partial volume effect is corrected. Thereafter, the final Population Module templates were created, ROI statistics were performed using MNI structural, Harvard-Oxford, Hammers, and custom atlases. Moreover, quality control procedures were included through inspection of image quality and rating quality as pass or fail [104].

Both the Aβ load and CBF in the whole brain and the following three regions of interest were calculated: (1) hippocampus, (2) posterior cingulate, and (3) precuneus. The first three ROIs were selected because they have been heavily affected by Alzheimer's

disease [105]. These regions are part of the focal neural modular network subserving episodic memory function and they substantially overlap with the default mode network [106]. It has been thought that higher lifetime cerebral metabolic stress associated with default activity across the individual's longevity span, may predispose these focal regions to AD-related alterations, including Aβ deposition and disruption of connections with the medial temporal lobe, leading to memory impairment [107].

5.2.7 Causation Analysis

The main parameters in our approach are serum cholic acid, Aβ in brain, and CBF. There may be association and correlation between them, nevertheless from a pathophysiological angle, we need to know is there any causational linkage between them, that is which parameter causatively affects which other. Knowing the causative parameter formulates a proper physiological basis of any process, and show which parameter is important from a physiological basis, thus indicating the path of possible therapeutic intervention. A standard mathematical procedure on temporal data is currently available [93, 108]. This analysis can delineate causative links between parameters, with diverse applications in physiology, pathology and clinical medicine [53, 109]. Indeed, Granger causality has been incisively applied on time-wise data, such as panel, longitudinal or cross-sectional data [110-112]. Granger causality analysis has been earlier well utilized to demarcate causative links between different brain signals (electrophysiological signals or neuroimaging signals), and is a robust procedure in neurophysiology and neuroradiology [109, 113]. We utilize Granger causation analysis [94] to uncover cause-effect relationships between our parameters and construct our equations below. We successively consider the causality relationship between (i) cholic acid and amyloid load (ii) cerebral blood flow and amyloid load.

5.2.7.1 Causality relationship between cholic acid and amyloid load

The association between serum cholic acid level (CA) and the amyloid load (SUVR) was then considered. We have taken the age-wise time series data for serum CA concentration and Aβ load. If amyloid deposit (SUVR) happens earlier than and influences cholic acid (CA), the former instigates and causes the latter, in the sense of mathematical causation analysis (Granger causality), which is a predictive causality. Likewise, another condition can be causality in the reverse direction: i.e., cholic acid instigates and causes amyloid load in the sense of Granger causality. We have investigated both the causation conditions separately using the following equations which we formulated from the causal dynamics analyzed by Thurman and Fischer (1988). In the equation below, we use the consecutive chronologically lagged time-points k = 1, 2, 3, 4 and 5, for testing Granger Causation in terms of test statistics to delineate the level of significance. We thus formulated the following equation denoting that the level of cholic acid causatively influences the level of amyloid load:

Causation equation for "Cholic acid → Amyloid load" effect:

$$CA_t = \mu + \sum_{k=1}^{p} \alpha_i \; CA_{(t-k)} + \sum_{k=1}^{p} \beta_k \; SUVR_{(t-k)} + \varepsilon_t \qquad (1)$$

This is a time-series equation from an autoregressive basis, incorporating a general linear regression model, whereby the value of a parameter now causatively depends on the situation upto k earlier time points (namely $t–1$, $t–2$, $t–3,\ldots,t–k$ whose cumulative effects are added by the summation symbol). As per the general linear model of regression analysis, the terms CA_t and ε_t respectively denote the baseline value of cholic acid and noise fluctuation. We now formulate likewise the reverse causation equation as below.

Causation equation for "Amyloid load → Cholic acid" effect:

Likewise, we formulated the reverse equation that the level of amyloid load causatively influences the level of cholic acid:

Causation equation for "Amyloid load → Cholic acid" effect:

$$SUVR_t = \mu + \sum_{k=1}^{p} \alpha_i \; SUVR_{(t-k)} + \sum_{k=1}^{p} \beta_k \; CA_{(t-k)} + \varepsilon_t \qquad (2)$$

To test whether amyloid load "SUVR" influences or causes cholic acid level "CA" or vice-versa, we estimated the variants (with different number of lags *k* in right side of both equation 1 and 2).

5.2.7.2 Causality relationship between amyloid load and cerebral blood flow

We then consider the possibility cause-effect relationship between amyloid load and cerebral flow. Similarly, we formulated the following equations:

Causation equation for "Amyloid load → Cerebral Blood Flow" effect:

$$SUVR_t = \mu + \sum_{k=1}^{p} \alpha_i \; SUVR_{(t-k)} + \sum_{k=1}^{p} \beta_k \; CBF_{(t-k)} + \varepsilon_t \qquad (3)$$

Causation equation for "Cerebral Blood Flow → Amyloid load" effect:

$$CBF_t = \mu + \sum_{k=1}^{p} \alpha_i \; CBF_{(t-k)} + \sum_{k=1}^{p} \beta_k \; SUVR_{(t-k)} + \varepsilon_t \qquad (4)$$

Regarding the evaluation of whether amyloid load "SUVR" influences or causes cerebral blood flow "CBF" or vice-versa, we assess the variants (with different number of lags *k* in RHS of equation 3 and 4).

5.2.8 Statistical Analysis

All statistical analyses were performed on Prism 8.0 for Windows (GraphPad). All data are expressed as Mean±SD (standard deviation). We tested the distributions of each variable for normality (using Anderson-Darling test). We found CBF and amyloid load (SUVR) to be normal distributions, hence the student unpaired t-test was used. On other hand, we found that MMSE and cholic acid were not normal distributions, so nonparametric assessment (Kolmogorov- Smirnov test) was utilized (see appendix). We assessed the linear association between amyloid load (SUVR) and CBF in control and AD subjects, using the correlation coefficient. Likewise, we obtained the correlation between amyloid load (SUVR) and MMSE, and also between CBF and MMSE. Further, the Z-score values of the variables were also found out for analyzing the inappterrelationships between serum cholic acid, CBF and amyloid load (SUVR).

A receiver operating characteristic (ROC) curve was generated for CN and AD subjects to determine the optimal cut-off value of CBF and SUVR of the whole brain and regions using Youden's J statistic index [114]. The index is defined for all points of a ROC curve, and the maximum value of the index is used as a criterion for selecting the optimum cut-off value. We obtained an additional important measure of the accuracy of the clinical test as the area under the ROC curve. This discrimination is reliable when sensitivity and specificity are close to 1.0, with minimal false positive and negative outcomes. Moreover, using power analysis methodology, we have calculated the minimum sample size needed for all our analyses, and the detailed calculation is presented in appendix, where we find that all our investigation well satisfies this sample size requirement.

5.3 Results

5.3.1 Serum cholic acid concentration in AD patients is half of normal subjects

This parameter is significantly altered in AD. We note that the mean cholic acid in Alzheimer patients is greatly diminished in compared to mean value in normal, and is only 46% of the average normal value. The Kolmogorov-Smirnov test revealed markedly significant alteration (p = 0.0487) in serum cholic acid levels in Alzheimer's subjects compared to normal individuals (Figure 25).

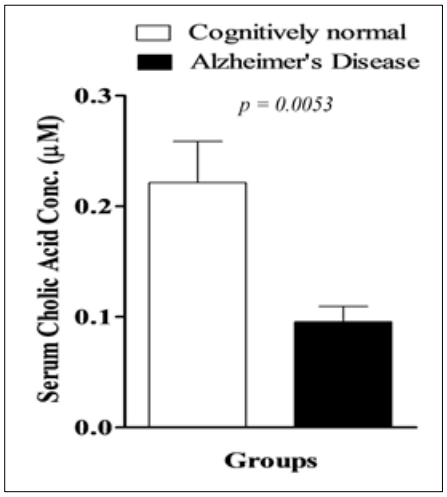

Figure 25: *Serum cholic acid level in Alzheimer's disease is less than half of normal subjects (statistical significance is substantial, with p = 0.0053).*

5.3.2 Cerebral blood flow in Alzheimer patients is half of normal subjects

We find that total and regional cerebral blood flow (hippocampus, precuneus, posterior cingulum) strongly decreases in Alzheimer's patients compared to cognitively normal subjects (p<0.0001) (Figure 26a). Actually, the mean blood flow in Alzheimer patients in all these regions is about half (≈45-55%) of normal subjects.

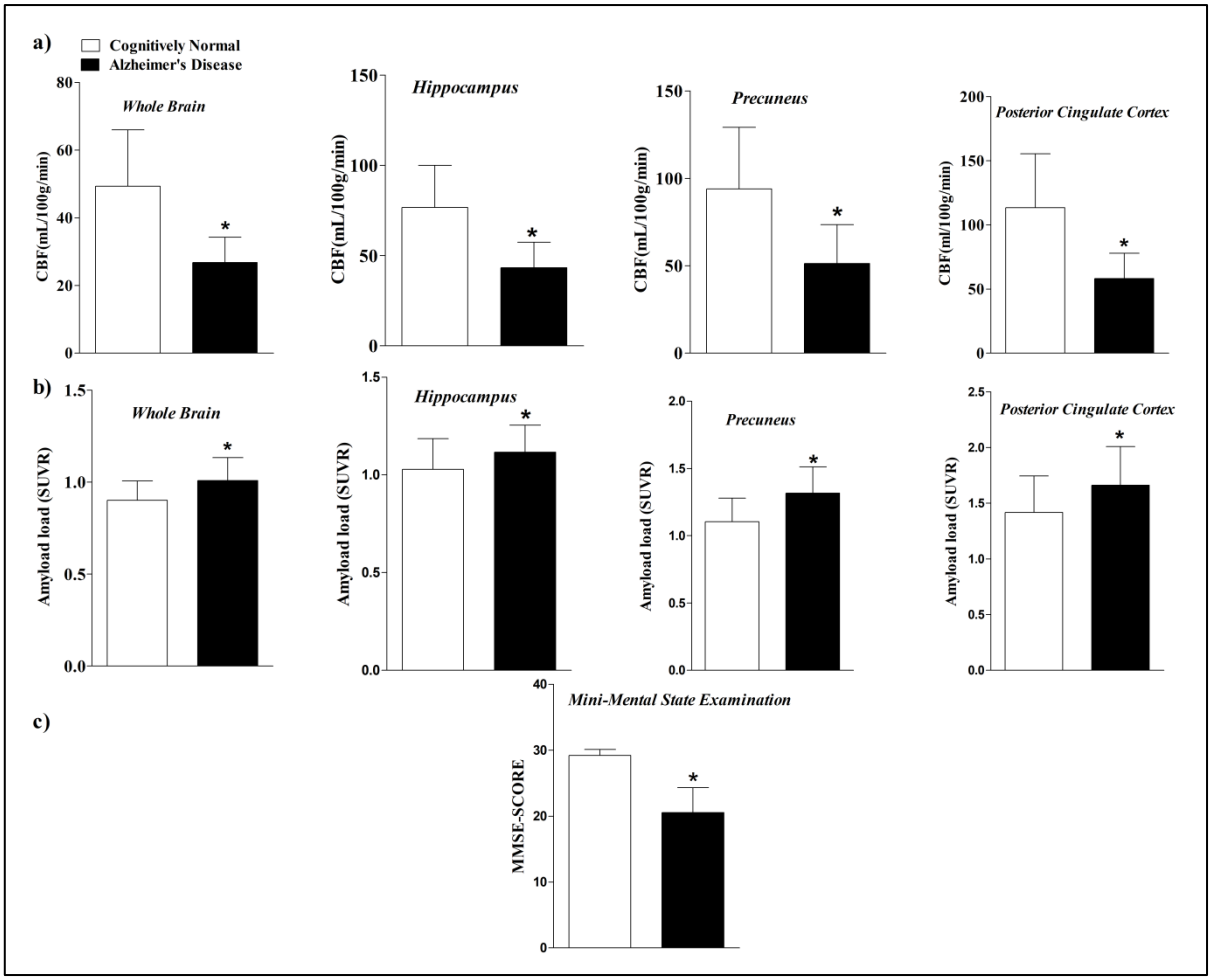

Figure 26: *Whole brain and region-wise cerebral blood flow (a), amyloid-load (b), and mini-mental state examination score (c), in normal individuals and Alzheimer's disease subjects. The statistical significance measure $p < 0.05$ when Alzheimer's disease group is compared with cognitively normal group for each of the nine figure panels.*

5.3.3 Higher amyloid-beta load in Alzheimer's disease

We have quantified amyloid-beta burden via standard uptake value ratio, which indicates a robust increase in amyloid load in the whole brain and precuneus ($p<0.0001$), posterior cingulate cortex ($p=0.0004$), and hippocampus ($p=0.0039$) in AD subjects compared to CN subjects (Figure 26b). Furthermore, the mini-mental state examination score is substantially lower in Alzheimer's subjects compared to normal ($p<0.0001$) (Figure 26c). Moreover, the increase of amyloid load in Alzheimer's subjects when compared to cognitively normal individuals across the whole brain and the different brain regions are represented with SUVR colorscale (Figure 27).

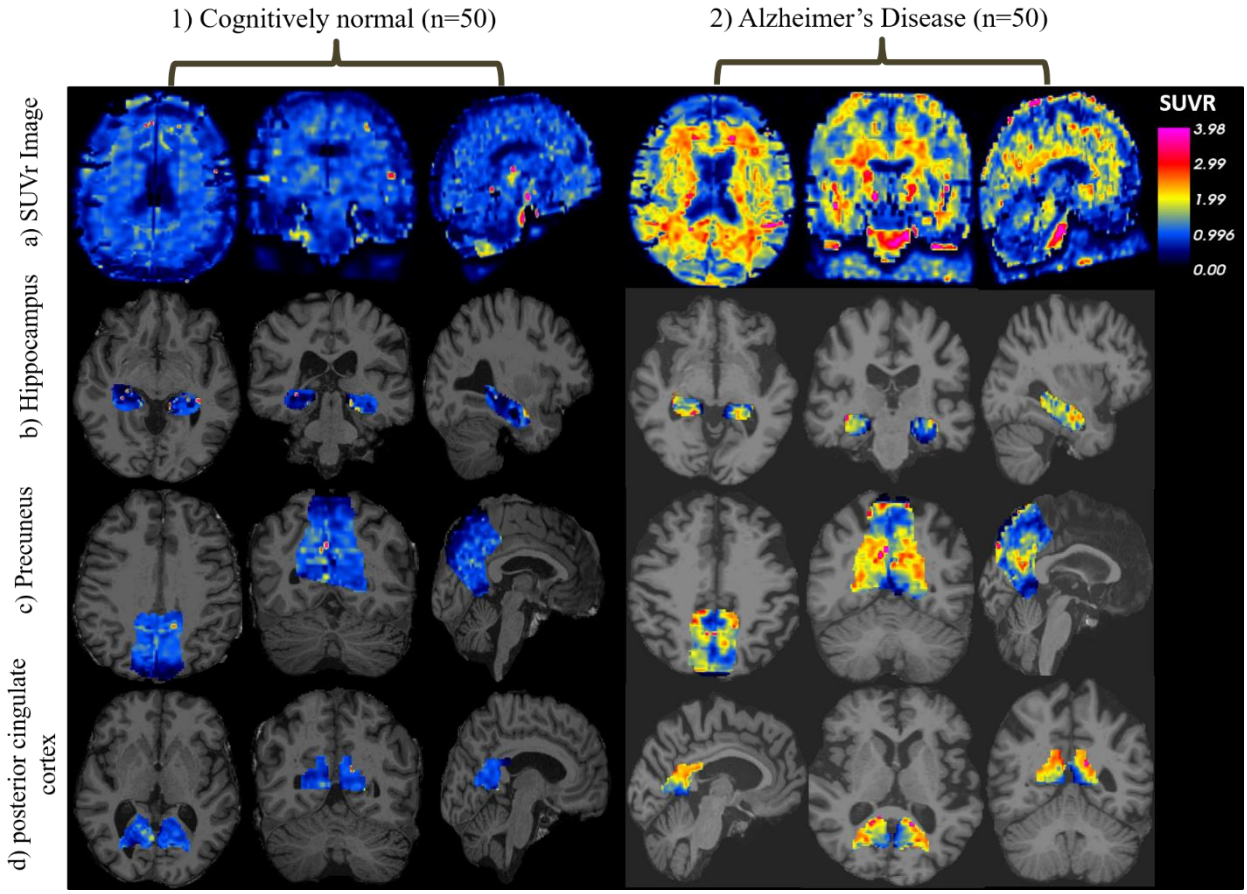

***Figure 27**: Differences in amyloid load (SUVR) displayed for PET images after correcting for partial volume effects (PVC). The figures are presented as SUVR colorscale; the value of amyloid deposition increases along the colour spectrum continuum: blue-yellow-red.*

5.3.4 Correlation between amyloid load (SUVR) and CBF with MMSE

Examination of simple main effects using non-parametric tests (Spearman's correlation) revealed there were significant negative association (ρ = -0.3126, p =0.0015) between whole brain amyloid load (SUVR) and MMSE score (Figure 28a). On the other hand, there were substantial positive association (ρ = +0.6446, p< 0.0001) between whole brain CBF and MMSE score (n=100) (Figure 28b).

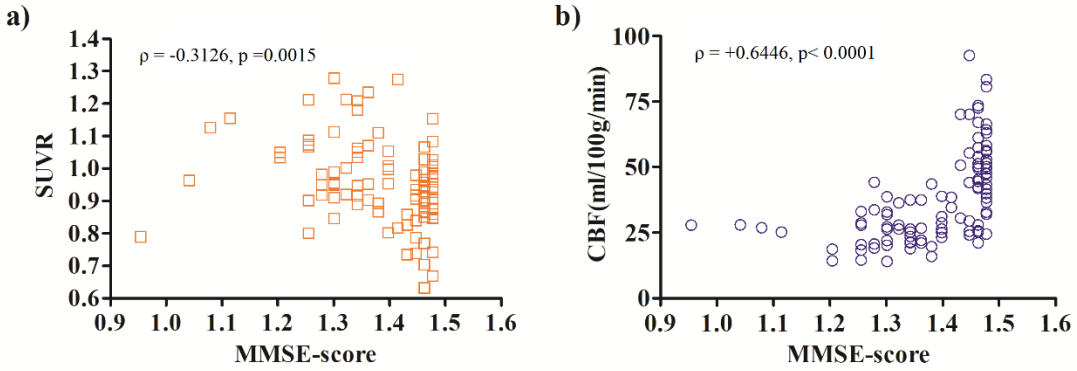

Figure 28: *Correlation between mini-mental state examination (MMSE) score with amyloid load (a), and with cerebral blood flow (b). There is negative correlation between amyloid load and MMSE (a), but positive correlation between cerebral blood flow and MMSE. All interactions were statistically significant (n=100, p < 0.05 in both cases).*

5.3.5 Receiver Operating Characteristics Curve

This ROC curve was generated for amyloid load (SUVR) and CBF in the whole brain and the other regions of AD and CN subjects. Implementing Youden's J statistic, the optimal cutoff value for amyloid load (SUVR) was obtained at 61% mean sensitivity, resulting in 78% mean specificity, the value being estimated in the whole-brain (0.9485 ml/100g/min), hippocampus (1.136 ml/100g/min), precuneus (1.159 ml/100g/min), and posterior cingulate (1.773 ml/100g/min) (Figure 29a and b). Similarly, the cutoff value was obtained at 91% mean sensitivity, resulting in 75% mean specificity regarding CBF, the cutoff value being found in whole-brain (39.38 ml/100g/min), hippocampus (66.38

ml/100g/min), precuneus (82.97 ml/100g/min), and posterior cingulate (73.46 ml/100g/min).

Furthermore, the area under the ROC curve is also an important index that can be used to determine which of the above-mentioned parameters (amyloid load or CBF) has the highest discrimination power among diseased and normal populations. Higher diagnostic accuracy of a parameter is measured by the AUC being close to 1, which suggests a high probability of true positives and a low probability of false negatives. Likewise, if the AUC is close to 0.5, it implies that the ROC curve is close to the line of identity at which there is no difference between the distributions of the values of the parameter in patients and in healthy volunteers, i.e., there is minimal diagnostic discrimination. In our study, the AUC values revealed that CBF estimation (when compared to SUVR estimation) has higher power of discrimination in the whole brain ($p< 0.05$), hippocampus ($p <0.001$), and posterior cingulate cortex ($p< 0.05$) among CN and AD. However, in the precuneus, the ROC areas or discrimination powers were not significantly different for the CBF and SUVR (Figure 29c). Our observation that the CBF has more discrimination power that SUVR can be elucidated by the ROC characteristics.

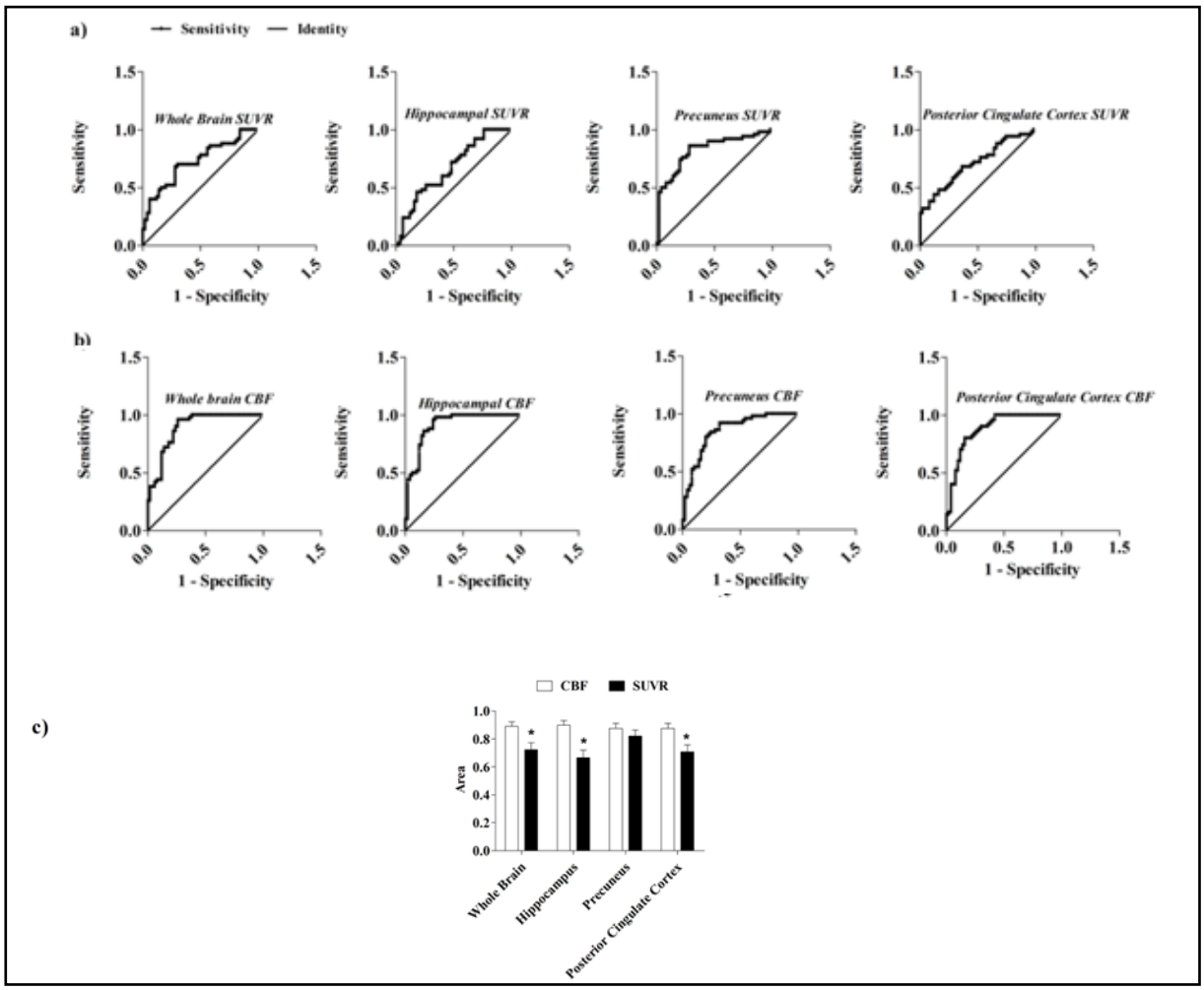

Figure 29: *Receiver-Operating Curves for amyloid load SUVR (a), cerebral blood flow CBF (b), and the Areas under the ROC curve (c) in the whole brain and ROIs (hippocampus, precuneus and posterior cingulate cortex) of normal individuals and Alzheimer's subjects. The sensitivity and specificity are calculated using Youden's J statistic for the ROC curves. In the vertical axis of panel (c), the value of area closes to 1 represents highest discrimination power of the parameter and lower values of area suggests less discrimination power, and indicates that the corresponding ROC curve in (a) or (b) is close to the diagonal line of identity at which there is possibility of least discrimination between healthy and diseased subjects.*

5.3.6 Interaction of Cholic acid, Amyloid beta and Cerebral blood flow

We have calculated z-score values of serum cholic acid concentration, amyloid load (SUVR), and CBF measurements obtained from the same subjects (n=30) and performed linear regression analysis to analyse the correlation among them. Regression analysis revealed there were significant interaction of serum cholic acid levels with amyloid SUVR [$F_{1,28}$= 4.213, p=0.0496, R^2=0.1308] and with CBF [$F_{1,28}$= 41.01, p< 0.0001, R^2=0.5943] (Figure 30).

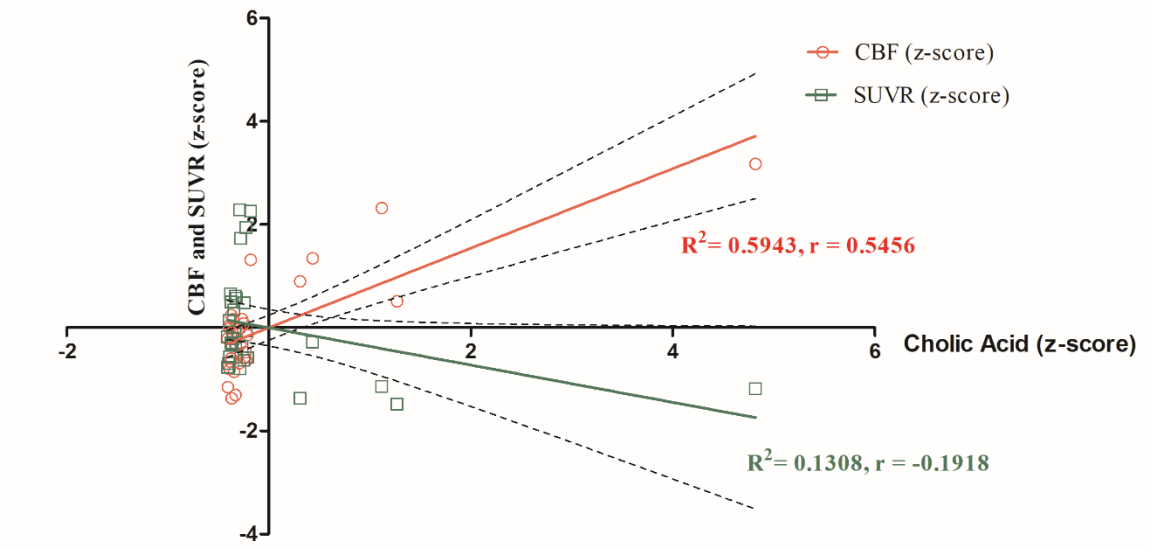

Figure 30: *Scatterplots of the interaction between serum cholic acid concentration with amyloid load (SUVR) and cerebral blood flow (CBF). All values are represented in z-scores and the interactions were statistically significant ($p < 0.05$).*

5.3.7 Cholic acid causatively influences Amyloid-β load

We then performed causation analysis by Granger methodology and observed that cholic acid influences amyloid load (SUVR), indicating that cholic acid impacts and actuates Aβ load with high significance (p=0.01; right side of Table 5). However, for the reverse condition that alteration in Aβ load causes alteration in cholic acid, we find that the $p > 0.05$ for all the lag values, thus indicating that this direction of causality is not significant and is untenable (p=0.06; left side of Table 4). Moreover, the symmetric regression analysis also revealed that the coefficients on lagged cholic acid levels were

significant (p = 0.0205) as a group compared to amyloid load (SUVR) coefficients which show non-significance (p = 0.1670). This lagged coefficient analysis further consolidates the causation effect, namely that considering the full gamut of time-lagged coefficients as a group, the cholic acid caused the amyloid load (p=0.0205), however the reverse causation (amyloid load causes cholic acid) is not valid as p>0.05 (as p=0.1670). Detailed analysis can be found in the appendix.

Table 4. F-test results for "Amyloid load causatively alters cholic acid" and "Cholic acid causatively alters amyloid load".

Amyloid load causatively alters Cholic acid			*Cholic acid causatively alters Amyloid load.*		
k = no. of lags	F-statistic	*p*-value	*k* = no. of lags	F-statistic	*p*-value
1	3.95	0.06	***1***	***7.63***	***0.01***
2	0.54	0.59	2	2.07	0.15
3	1.11	0.37	3	1.50	0.25
4	0.77	0.56	4	1.28	0.32
5	0.49	0.78	5	0.85	0.54

5.3.8 Amyloid load causatively influences Cerebral blood flow

We used Granger test to reveal that alteration in Aβ load causes alteration in Cerebral blood flow (p=0.02; right side of Table 5) suggesting that Aβ load impacts and actuates cerebral blood flow. However, Granger test also shows that the reverse causation, namely that cerebral blood flow influences Aβ load, is untenable (p > 0.05; left side of Table 6). Furthermore, the symmetric regression analysis also revealed that the coefficients on lagged amyloid load (SUVR) were significant (p = 0.023529) as a group compared to cerebral blood flow coefficients which has non-significance (p = 0.064682). Detailed analysis could be found in the appendix.

Table 5. F-test results for "Cerebral blood flow causatively alters Amyloid load" and "Amyloid load causatively flow alters Cerebral blood".

Cerebral blood flow causatively alters Amyloid load			*Amyloid load causatively alters Cerebral blood flow*		
k = no. of lags	F-statistic	*p*-value	*k* = no. of lags	F-statistic	*p*-value
1	2.48	0.13	1	1.82	0.19
2	0.44	0.65	2	1.51	0.24
3	0.40	0.75	3	2.43	0.10
4	0.24	0.91	4	1.69	0.20
5	0.12	0.98	5	0.83	0.55
6	0.62	0.71	6	2.97	0.06
7	0.57	0.76	***7***	***5.03***	***0.02***

5.3.9 Mechanistic substantiation of inhibition of amyloid-β formation by cholic acid

We now consider the first causal connectivity: "cholic acid→amyloid". It has been experimentally observed that treatment with oral cholic acid derivative can decrease amyloid-beta ($A\beta_{1\text{-}40}$, $A\beta_{1\text{-}42}$) and amyloid-precursor protein (APP) in brain (cerebral cortex and hippocampus) in rodent preparations [118], where Aβ diminished prominently to 32%-66% of the Aβ level in hippocampus and frontal cortex in the pre-treatment group. Additionally, it has been empirically found that cholic acid derivative can abrogate amyloid-produced synaptic toxicity in mice models, which as estimated by postsynapsin-95 marker [119]. Moreover, it has also been revealed [87] that cholic acid can avert cognitive impairment and amyloidogenic propensity in APP/PS mice under senescent changes. Actually, one knows from preclinical studies [118] that the pharmacological cholic acid derivative (Tauroursodeoxycholic acid, TUDCA) strongly downregulates (> 10 fold) the CGTF (connective tissue growth factor) gene, substantially decreasing the

expression of CTGF protein, which in turn diminishes γ-secretase activity, thus decreasing APP processing and lessening amyloid production (Figure 31).

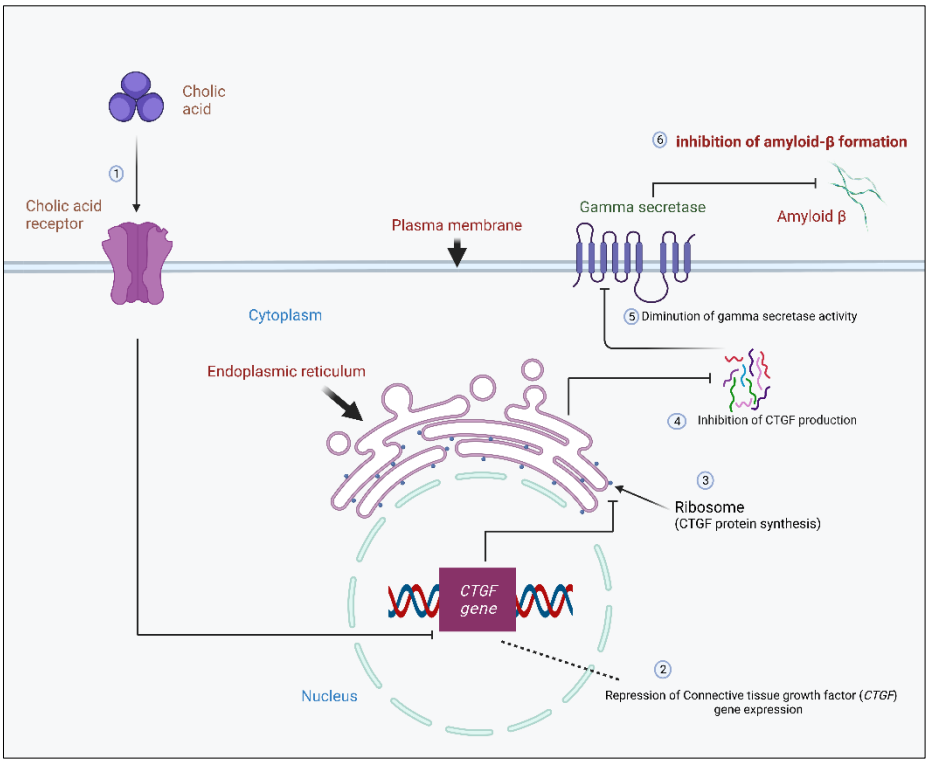

Figure 31: *Animal Experimentation-based mechanistic validation of the mathematically-predicted causation relationship: Cholic acid inhibits Amyloid beta formation. The biochemical pathways are obtained from the rodent investigations.*

5.3.10 Mechanistic corroboration of inhibition of cerebral blood flow by amyloid-β

Here we attend to the second causal connectivity: "amyloid→CBF". Our causation methodology delineates that Aβ-level influences and affects cerebral blood flow. This can be accounted for by the observation that amyloid deposit produces reactive cerebral amyloid angiopathy, whereby the deposit attaches with and obstructs the perivascular valves and periarteriolar circulation [120]. Actually, the amyloid of the brain tissue interstitial space contigously extends around and into the capillary space, thus furnishing the substrate of perivascular valvular obstruction. Additionally, amyloid toxicity can also produce pericyte activation and contactility around the capillaries, further decreasing the blood perfusion [121]. All these can decrease the blood transport through brain tissue, thus diminshing the cerebral blood perfusion and flow (Figure 32).

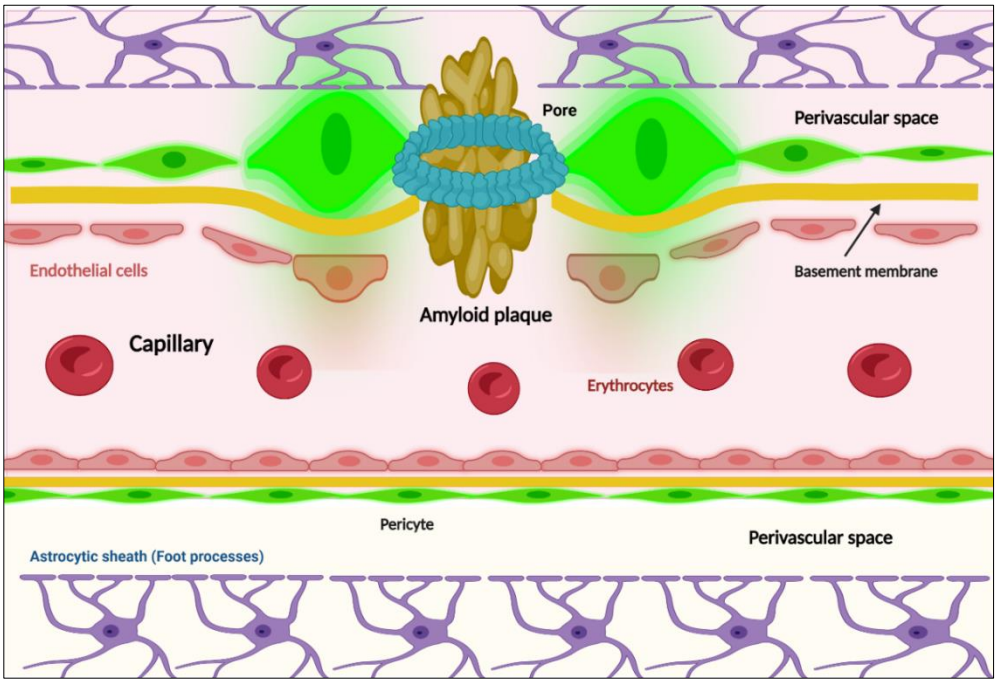

Figure 32: *Preclinical experimental corroboration of the predicted causality linkage: increasing amyloid beta inhibits cerebral blood flow. The biophysical changes shown in the figure are observed in the animal studies.*

5.3.11 Normal subjects - Relationship of Mental status with Aβ load and with CBF

Our regression analysis revealed that there was no significant relation between age and mini-mental state examination score with Aβ load in cognitively normal subjects (Figure 33a, b).

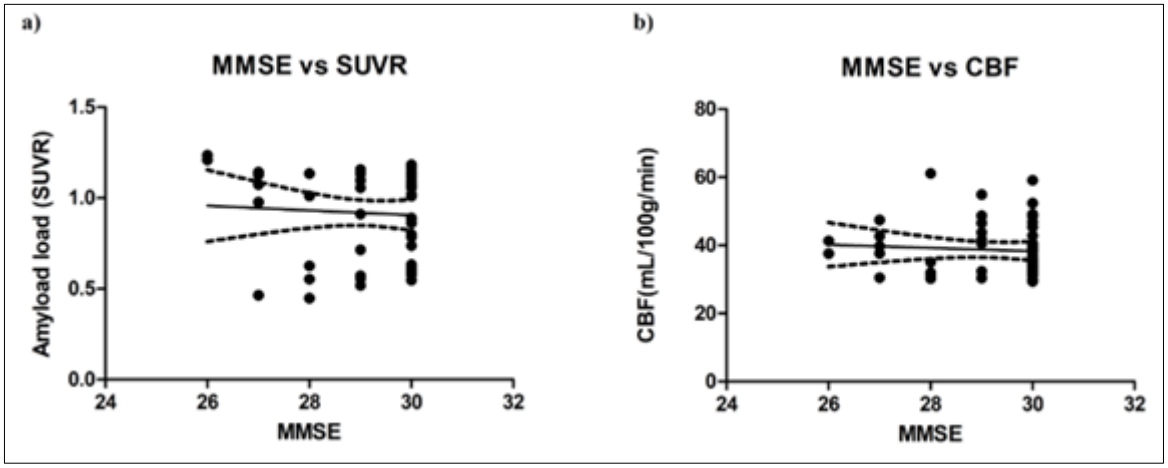

Figure 33: *Relationship of mini-mental state examination MMSE score with amyloid-beta load SUVR (a), and with cerebral blood flow CBF (b) in normal subjects, showing the best-fit (solid) regression line, with 95% CI (dotted) in all subjects (n=50). There was no correlation of MMSE with amyloid-beta load or with CBF in normal subjects (MMSE vs SUVR: $r^2 = 0.004072$, $p = 0.6598$; MMSE vs. CBF: $r^2 = 0.005026$, $p = 0.6247$).*

5.3.12 Relationship of Amyloid load to Cerebral Blood Flow in Normal subjects

We compared the relationship between CBF and Aβ load in cognitively normal subjects for whole brain (WB) and three important brain regions affected in Alzheimer's disease namely hippocampus (Hip), precuneus (PC) and posterior cingulated cortex (PCC). We found there was no significant correlation (Figure 34a-d).

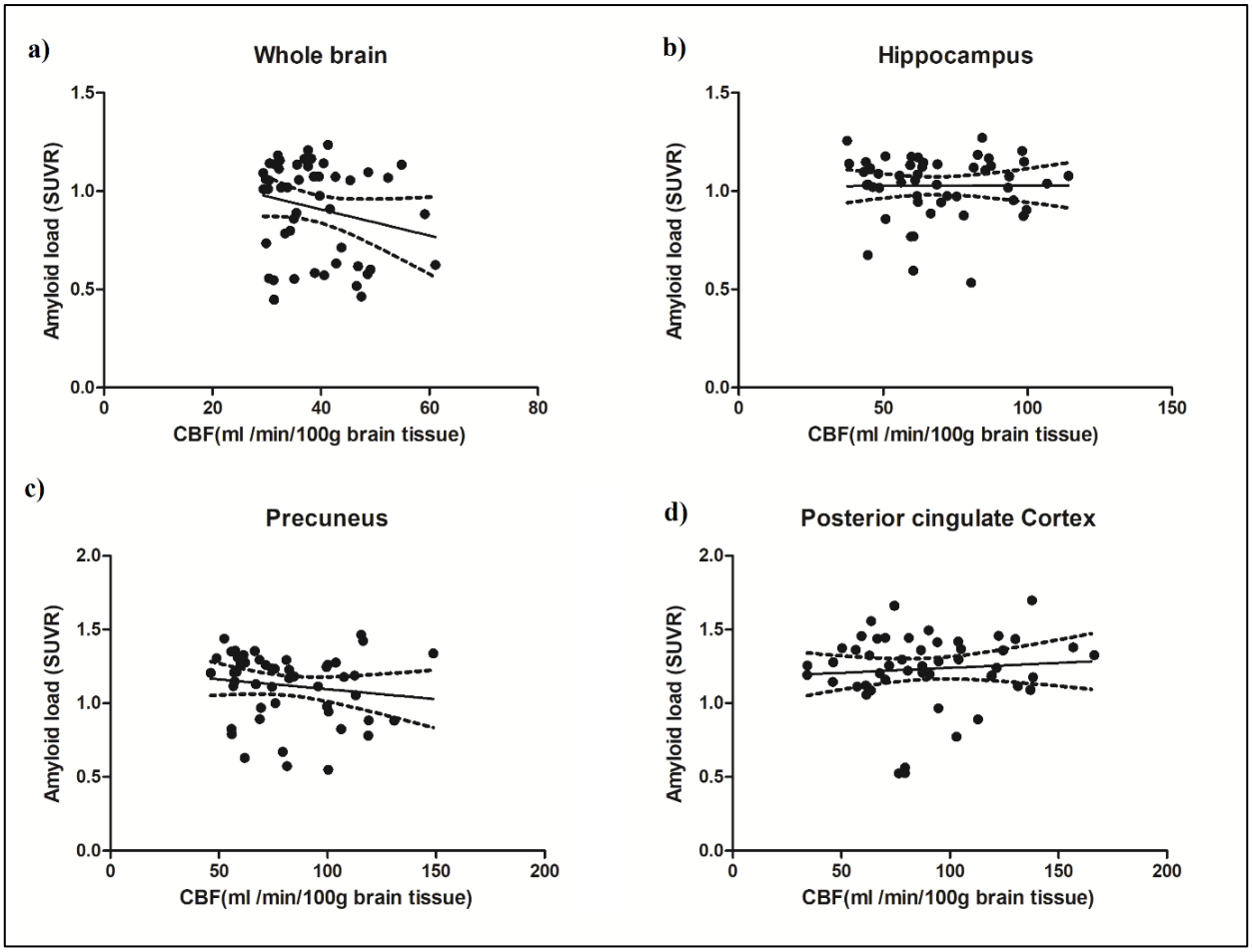

Figure 34: *Relationship between amyloid-beta load and cerebral blood flow in normal subjects: (a) Whole brain, (b) Hippocampus, (c) Precuneus, and (d) Posterior cingulated cortex (PCC), showing best-fit (solid) regression line and 95% confidence interval CI (dotted) in all subjects (n = 50). There was no correlation between amyloid-beta load and cerebral blood flow in any of the panels (Whole brain: $R^2 = 0.04796$, $p = 0.1265$; Hippocampus: $R^2 = 0.00004149$, $p = 0.9646$; Precuneus: $R^2 = 0.02014$, $p = 0.3256$; Posterior cingulate cortex: $R^2 = 0.007070$, $p = 0.5615$).*

We now consider the aforesaid lack of significant correlation between amyloid load and CBF for normal subjects. Thus, even if amyloid load increases, it will have no effect on cerebral blood flow. It may be noted that the amyloid level in normal subjects is significantly lower that Alzheimer subjects (section 5.3.3), and we can consider normal subjects as being in lower-amyloid regime. On the other hand, Alzheimer's subjects are in higher-amyloid regime, having higher amyloid (section 5.3.3). Furthermore, in Alzheimer's subjects, higher level of amyloid load causatively decreases CBF (section

5.3.4). We thus observe that here a threshold concentration effect whereby if the amyloid load is in the lower regime, then there is no detrimental effect on cerebral blood flow; however, if the amyloid load is in the higher regime, there ensues the pathological situation of low cerebral blood flow.

5.4. Discussion

5.4.1 Primary findings

In the present study, we investigated the potential influence of cholic acid, a primary bile acid, on Alzheimer's disease, and cognitive impairment. Regarding Alzheimer's subjects. we have analysed the serum cholic acid (CA) concentration from Alzheimer's Disease Neuroimaging Initiative program's cohort (ADNI) studies and found that in these patients, there was a significant reduction in CA levels compared to normal subjects. Our study revealed that decreased cholic acid levels could cause an increase of amyloid beta load in the brain, and the increased amyloid beta load can cause a diminution in cerebral blood flow. Accordingly, we also found correlation between cholic acid level, Aβ load, and cerebral blood flow. Interestingly, on the other hand, regarding normal subjects, we could not find any correlation between amyloid load and cerebral blood flow for cognitively healthy controls, which may be due to a subthreshold process of biochemical kinetics.

Furthermore, we observed that amyloid load in the patients increased considerably in the brain regions, which were more affected in AD, such as hippocampus, precuneus, and posterior cingulate cortex. Indeed, these findings are also cross-validated in an independent study [122]. To underscore, it has also been reported that the precuneus is a highly vulnerable region for amyloid-beta deposition compared to other cortical regions [123].

5.4.2 Alteration of cholic acid level influences cognitive impairment

Our study revealed that cholic acid (CA) level was significantly diminished in Alzheimer's subjects compared to healthy subjects. Reduction of CA level indicatesthat cholesterol metabolism is abnormal as cholic acid is the primary metabolite of cholesterol [124]. Several reports suggest that the whole body's cholesterol metabolism is affected by ageing [89] and there is a pathogenic link between dysregulation of cholesterol metabolism with Alzheimer's disease [125]. Given that cholic acid is the primary by-product of cholesterol in this context, and as per reactant-product interaction dynamics, an increase in cholic acid production would indicate a decrease in the quantity of cholesterol. Simons et al. reported that by depleting cellular cholesterol levels in hippocampal neuron, the formation of amyloid beta was completely inhibited [126]. Therefore, cholic acid, an important biomarker for cholesterol metabolism, reveals a significant link of bile acid metabolism with cognitive impairment.

5.4.3 Cholic acid as causative factor in decreasing Amyloid load

We have observed that serum cholic acid is markedly decreased in Alzheimer's subjects when compared to normal subjects (sec. 5.3.1). Furthermore, we noted that amyloid load is substantially increased in Alzheimer's patients with respect to healthy controls (sec. 5.3.3). In other words, serum cholic acid is inversely related to amyloid load. We found that this inverse relationship is actually a causative relationship by means of causality analysis, indicating that increased serum cholic acid actuates decreased amyloid load in brain. This behaviour transpires to be substantiated by collateral preclinical studies. To illustrate, it has been experimentally observed that treatment with oral cholic acid derivative can decrease amyloid-beta ($A\beta_{1\text{-}40}$, $A\beta_{1\text{-}41}$) and amyloid-precursor protein (APP) in brain (cerebral cortex and hippocampus) in rodent preparations [118], where Aβ

diminished prominently to 32%-66% of the Aβ level in hippocampus and frontal cortex in the pre-treatment group.

5.4.4 Amyloid beta causatively affects and inhibits cerebral blood flow

To recapitulate, we have seen that in Alzheimer's disease there is considerable diminution in cerebral blood flow (CBF) (sec. 5.3.2), and the disease process is associated with enhanced amyloid load (sec. 5.3.3). This indicates that amyloid beta load and CBF are reciprocally related. Likewise, further corroborates this reciprocity, namely the amyloid diminution is linked with CBF increase. Our causality analysis procedure elucidates that the linkage is a causation, whereby amyloid escalation produces CBF reduction.

5.4.5 Healthy subjects: No relationship between amyloid load and cerebral blood flow. Concentration Threshold effect

To delineate whether amyloid load and CBF are related in healthy normal subjects, we have performed a correlation analysis which failed to decipher any significant correlation between CBF and amyloid load for normal subjects (section 5.3.11). Thus, even if amyloid load increases, it will have no effect on cerebral blood flow. This is in contrast to Alzheimer's subjects, where increase of amyloid load (section 5.3.3) causatively decreases CBF (section 5.3.2), thus posing a divergent behaviour with respect to the situation in normal subjects. We can clarify this divergent behaviour of amyloid in the two regimes by using the concept of "threshold concentration effect" in biochemistry and toxicology.

We assess the effects of the neurotoxic behaviour of amyloid protein from a kinetics perspective. As per the observation of "concentration threshold effect" in toxicology, a minimum level of a substance is required to show toxicity manifestation [127]. Such threshold concentration effect has also been well observed in neurodegenerative disorders as Huntington's disease. Here a minimum threshold

concentration of the toxic protein Huntingtin is required for the concretion formation and cellular toxicity [128]. It may likewise be taken that one needs an accumulation of amyloid to a threshold level for deleterious effect to be manifested. Hence, in normal individuals the amyloid concentration is in the lower regime, though the level may vary between individuals, nevertheless the detrimental effect as CBF reduction may not occur (subthreshold effect). However, in Alzheimer's patient, the amyloid concentration is in the higher regime, and thus the hazardous effect of CBF reduction would occur (suprathreshold effect).

Our study is also corroborated with previously reported findings [129], where it has been also shown there was no significant association between CBF and cognition for healthy subjects, nevertheless it may be noted that our sample size is about five times that of the cited paper. As mentioned above, we have accounted for these two divergent anomalous behaviours that we observe in Alzheimer's vis-à-vis normal subjects, by using the biochemical and toxicological principle of the Threshold Concentration Effect. We thus found that the cerebrovascular deleterious behaviour of amyloid transpires to be a threshold effect from a toxicological basis.

5.4.6 Diagnostic and therapeutic implications

We have shown that decreased serum cholic acid plays an incisive role in the accentuation of amyloid load in Alzheimer's disease where cholic acid level diminishes to about 40-45% of normal subjects. Indeed, monitoring serum cholic acid level may enable a cost-effective implementation of preventative initiatives and screening methodology for the general population. This measurement should be supported by specific confirmatory diagnostic tests to prevent false positives/false negatives. The estimation of serum cholic acid or biliary profile, may be a useful as a pre-screening tool or tracking technique to demarcate those at high risk of developing Alzheimer's disease, and thereby, prophylactic,

prognostic or disorder-modifying intervention can be undertaken to retard the disease-progression.

We have shown that lower serum cholic acid has a determining causational factor in Alzheimer's disease. Hence this indicates a possible role of using cholic acid (or its common pharmacological derivatives as tauroursodeoxycholic acid) as a therapeutic intervention of Alzheimer's disease. This approach may be further vindicated by the fact that cholic acid has already been successfully used as therapeutic intervention in neurodegenerative diseases. For instance, tauroursodeoxycholic acid (TUDCA) well ameliorated the motor symptoms in a preclinical trial of Parkinson's disease. Moreover, a clinical study has reported the efficacy of TUDCA in amyotropic lateral sclerosis patients.

Additionally, another cholic acid agent (ursodeoxycholic acid, UDCA) was also reported to be safe and tolerable in Parkinson's disease patients[130]. Furthermore, in several behavioral experimental investigations in preclinical trials of AD using chenodeoxycholic acid (CDCA) showed substantial improvement in spatial memory and cognition [131]. Table 7 highlights the results of various investigational studies of cholic acid and derivatives elucidated above. To paraphrase, the aforesaid evidence well points out the therapeutic potency of cholic acid in AD. The above-mentioned cholic acid based novel therapeutic intervention needs to be developed well as a compelling clinical strategy, especially as neurologically centred therapies of may be unable to fully give benefits to the desired level.

Table 6. Summary of trials regarding cholic acid and cholate modulator derivatives.

Structure	Candidate agent	Clinical/ Preclinical Study	Observations	References
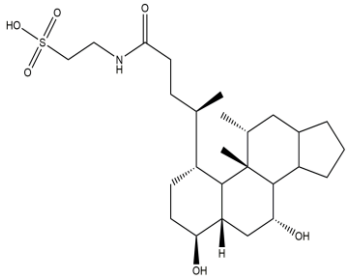	Tauroursodeoxy-cholic acid	Human	Retardation of disease progression (*n*= 320)	[132]
		Human	Neuropathic impairment score stabilized; further decline halted (*n* = 20)	[133]
		Rodent	Decrease of amyloid-load in brain (*n*= 17)	[118]
		Murine	Reduction of amyloidogenic propensity and enhancement of cognitive performance (*n*= 50)	[87]
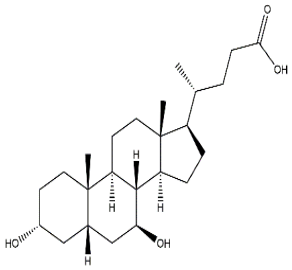	Ursodeoxy-cholic acid	Human	Retardation in the decline of speech and motor functions (*n* = 53)	[134]
		Human	CSF penetration of drug satisfactory, low side-effects, sufficient tolerability (*n* = 18)	[135]
		Human	Good endurance to the drug (*n* = 30)	[130]
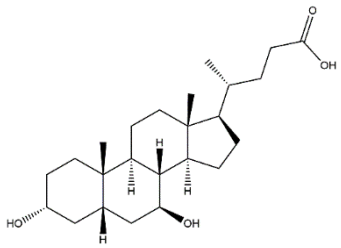	Cholic acid	Human	Delineation of metabolic cholic profilefor AD (*n*=141)	[124]
		Murine	Suppression of amyloid-induced synaptic damage in AD (*n*= 7)	[119]
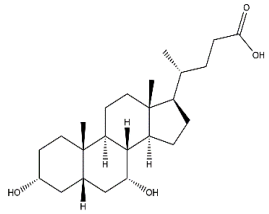	Chenodeoxy-cholic acid	Rats	Memory and cognition enhancement in AD (*n*=13)	[131]

Total number: Human subjects = 582, Animal preparations = 87.

5.5 Conclusion

In this chapter, we have approached Alzheimer's disease from its basic pathophysiological operation, namely as a hepatic metabolic dysfunction. We provide attention to basic hepatobiliary metabolite, as bile acid, where cholic acid is a primary constituent. With this perspective, we find that serum cholic acid in AD falls to half of that in normal subjects. Moreover, brain amyloid load in AD is significantly higher than normal subjects. Further, total and regional cerebral blood flows in AD substantially decreases by 45-50% of normal values. We show that serum cholic acid decline can be a major factor in AD, and can causatively increase brain amyloid. Our findings indicate that this higher amyloid load in turn can causatively diminish cerebral blood flow in AD patients. In contrast, for normal subjects, we find that amyloid level changes have no influence on blood flow. This may be due to the principle of threshold concentration effect in toxicology, where concentration of a toxic factor (as amyloid) needs to exceed a threshold level for producing a deleterious manifestation (as blood flow decrease).

We utilized causation analysis methodology to elucidate the underlying dynamics that may actuate the predisposition of Alzheimer's disease. We found the following causal chain: Cholic acid level → Amyloid load → Cerebral blood flow, where serum cholic acid inhibits amyloid formation, and this lessening of amyloid can decrease arteriolar constriction in brain tissue, thus increasing the cerebral blood flow. The aforementioned causation chain, furnished by our causality analysis, was corroborated by using findings from collateral in-vitro experimental animal studies. Further the causation analysis procedure indicated the potentiality of using cholic acid derivatives as possible repositioned pharmaceuticals to alleviate AD. Here also, overall analysis of the collateral clinical trial observations substantiated the potential efficacy of the predicted drugs, as cholate derivatives [136, 137]. Thus, we note that the causation analysis approach can give

mechanistic insights that may have the innovative possibility of impactful prospects in etiopathological and therapeutic applications in the clinic.